



Article

Synthesis of an NaY zeolite molecular sieve from a kaolin/dimethyl sulfoxide intercalation composite

Shu-Qin Zheng^{1,2*}, Ou Chen¹, Si-Cheng Liu¹, An Li^{1,2}, Li-Jun Li^{1,2}, Yong-Bing Yuan^{1,2} and Ceng Zhang^{1,2}

¹Department of Chemistry and Chemical Engineering, Hunan Institute of Science and Technology, Yueyang 414006, Hunan, China and ²Hunan Province Key Laboratory of Speciality Petrochemicals Catalysis and Separation, Yueyang 414006, Hunan, China

Abstract

NaY zeolite was synthesized from kaolin/dimethyl sulfoxide (DMSO) intercalation composites using an *in situ* crystallization technique. The effects of the intercalation ratios and the amounts of the kaolin/DMSO intercalation composite on the synthesis of an NaY zeolite molecular sieve were studied. The samples were characterized by X-ray diffraction, Fourier-transform infrared spectroscopy, differential thermal analysis, N₂ adsorption–desorption and scanning electron microscopy. In the *in situ* synthesis system, when the kaolin/DMSO intercalation composite was added, pure NaY zeolite was formed. By increasing the amount of kaolin/DMSO intercalation composite added, the crystallinity of the samples increased, and after reaching the maximum amount of kaolin/DMSO intercalation composite added, the crystallinity decreased with further increases of the amount of kaolin/DMSO intercalation composite added. To higher intercalation ratio, the crystallinity can be greatly improved at the lower addition content. At an intercalation ratio of 84%, the added amount of kaolin/DMSO intercalation composite was 2.5% and the crystallinity of the NaY zeolite molecular sieve reached a maximum value of 45%. At intercalation ratios of 55% and 22%, the amount of kaolin/DMSO intercalation composite added was 15% and the crystallinities of the NaY zeolite molecular sieves were 44% and 47%, respectively. The NaY zeolite has good thermal stability and a particle diameter of ~0.5 μm. The Brunauer–Emmett–Teller (BET) specific surface area and pore volume of the sample were 519 m² g⁻¹ and 0.355 cm³ g⁻¹, respectively.

Keywords: DMSO, *in situ* technique, intercalation composite, kaolin, NaY zeolite

(Received 21 August 2020; accepted 1 February 2021; Associate Editor: Saverio Fiore)

Zeolites are Al-silicate minerals with a three-dimensional framework structure of tetrahedral units that have abundant micropores of molecular dimensions. The zeolites are widely used as catalysts, ion exchangers and molecular sieves in the petrochemical industry and as adsorbents in separation and pollutant purification owing to their channel structure and remarkable adsorption performance (Chen *et al.*, 1986; Sang *et al.*, 2019; Chen *et al.*, 2020; Qiu *et al.*, 2020).

NaY zeolite is the most significant, mass-produced zeolite that can be prepared using a conventional gel synthesis method or *in situ* crystallization. In the latter technique, the NaY zeolite is crystallized into/onto clay matrices, which enhances their thermostability (Harding *et al.*, 2001; Wang *et al.*, 2007; Xiong *et al.*, 2015; Zhang *et al.*, 2019).

Kaolin is a clay composed mainly of the mineral kaolinite with a chemical composition of Al₂Si₂O₅(OH)₄. Kaolinite has a layered structure consisting of layers bound by hydrogen bonds (Cheng *et al.*, 2012; Castrillo *et al.*, 2015). Kaolinite can directly intercalate various organic molecules such as dimethyl sulfoxide (DMSO), urea, potassium acetate, formamide, N-methylformamide, ammonium acetate, etc. (Ledoux & White., 1966; Olejnik *et al.*, 1968; Adams, 1978; Tsunematsu & Tateyama, 1999; Cheng *et al.*, 2010; Makó *et al.*, 2014; Kovács & Makó, 2016). Kaolinite

intercalation composites not only have unique adsorption, dispersion, rheology, porosity and surface acidity, but also possess the functional groups and reaction activities of organic compounds. These composites have attracted the attention of researchers, such that the formation, structure and properties of kaolinite/organic intercalation composites have been widely investigated and discussed (Frost *et al.*, 1998; Kuroda *et al.*, 1999; Itagaki *et al.*, 2001; Matsumura *et al.*, 2001; Valaskova *et al.*, 2006; Matusik & Kłapyta, 2013; Cheng *et al.*, 2015, 2018; Makó *et al.*, 2016; Li *et al.*, 2017; Kristóf *et al.*, 2018).

In this work, we combine the *in situ* crystallization approach with kaolin intercalation. In this manner, NaY zeolite/kaolin composites with a zeolite content >40% could be obtained that utilize the functional groups and reaction activities of organic compounds.

Therefore, this work has focused on NaY molecular sieve synthesis using an *in situ* crystallization technique with kaolin/DMSO intercalation composites. The kaolin/DMSO intercalation composites was prepared using the direct intercalation method. The effects of the intercalation ratios and the amounts of added kaolin/DMSO intercalation composite on the synthesis of NaY zeolite molecular sieves were investigated.

Experimental

Raw materials

The materials used for the synthesis of the NaY zeolite were kaolin (China Kaolin Company), DMSO (Tianjin Komeo

*Email: zhengshuqin37@163.com

Cite this article: Zheng S-Q, Chen O, Liu S-C, Li A, Li L-J, Yuan Y-B, Zhang C (2021). Synthesis of an NaY zeolite molecular sieve from a kaolin/dimethyl sulfoxide intercalation composite. *Clay Minerals* 56, 28–36. <https://doi.org/10.1180/clm.2021.10>

Chemical Reagent Co. Ltd, AR), water glass (Changsha Wanfang Chemical Co. Ltd, $W_{\text{SiO}_2} = 20.9\%$, $W_{\text{Na}_2\text{O}} = 6.8\%$), sodium hydroxide (Tianjin Chemical Reagent Factory, reagent purity $\geq 98\%$, AR) and sulfuric acid (Tianjin Chemical Reagent Factory, reagent purity $\geq 98\%$, AR).

Preparation of the kaolin/DMSO intercalation composite

The DMSO was mixed evenly with kaolin at a $W_{\text{DMSO}}:W_{\text{kaolin}}$ ratio of 1:8 under stirring. The kaolin/DMSO intercalation composite was obtained by filtration, washing and drying after heating at 70°C for 24 h (sample denoted as KDM). The intercalation ratios of the samples were calculated using X-ray diffraction (XRD) according to the formula :

$$Q = I_{i(001)} / (I_{k(001)} + I_{i(001)})$$

in which Q is the intercalation ratio and $I_{i(001)}$ and $I_{k(001)}$ are the intensities of the (001) peak of kaolinite after intercalation and of the non-intercalated kaolin, respectively.

De-intercalation of the kaolin/DMSO intercalation composite

The de-intercalation reaction of the above intercalation composites was carried out after calcination at 40, 50, 60, 70, 80, 90, 100, 110, 120, 130, 140, 150, 160, 170, 180, 190 and 200°C for 2 h.

Synthesis of NaY zeolite molecular sieves using in situ technology

Kaolin, sodium silicate and distilled water were mixed thoroughly and sprayed, acquiring microspheres with average particle sizes of $\sim 75 \mu\text{m}$ in diameter. The microspheres were calcined at $950\text{--}980^\circ\text{C}$ for 2–3 h and at $700\text{--}800^\circ\text{C}$ for 2–3 h. The calcined microspheres were mixed with sodium silicate, sodium hydroxide, zeolite initiator and distilled water and the mixture was heated at $95\text{--}98^\circ\text{C}$ for 24–30 h to synthesize the composite. After the synthesis, the composite was washed, filtered and dried (sample denoted as R-NaY).

Synthesis of NaY zeolite molecular sieves by introducing KDM

The synthesis of NaY zeolite in this set of experiments followed the experimental procedure given in the previous section except for the use of KDM formed by intercalation of DMSO with kaolin. The amounts of added KDM were 1.0%, 2.5%, 5.0%, 10.0%, 15.0%, 20.0% and 25.0%, with the percentage referring to the KDM:calcined microspheres ratio. The NaY molecular sieves synthesized by introducing KDM was denoted as D-NaY.

Characterization of the synthesis products

XRD analysis

The crystallinity and crystal shape of the NaY zeolites were recorded on a Rigaku Ultimi IV diffractometer using $\text{Cu-K}\alpha$ radiation ($\lambda = 1.54056 \text{ \AA}$, 40 kV, 30 mA) with a scanned speed of $0.2^\circ \text{ min}^{-1}$. The crystallinity of reference NaY zeolite was equal to 93.1% and was denoted as S-NaY. The crystallinity of NaY zeolite was estimated according to the following equation:

$$\text{crystallinity (\%)} = \frac{\text{peak height at } 22.0\text{--}24.5^\circ 2\theta \text{ (product)}}{\text{peak height at } 22.0\text{--}24.5^\circ 2\theta \text{ (reference)}} \times 100$$

N_2 adsorption-desorption analysis

The specific surface areas, pore volumes and pore-size distributions were measured on an ASAP 2020 sorptometer (Micromeritics, USA) using adsorption and desorption isotherms collected at 77 K. Prior to the measurement, the samples were degassed at 373 K for 12 h. The specific surface areas were calculated using the Brunauer–Emmett–Teller (BET) method. The micropore volumes and external surface areas of the zeolite samples were calculated using the t-plot method. The pore parameters, mesopore surfaces and mesopore volumes were calculated from the desorption branches of these isotherms using the Barrett–Joyner–Halenda (BJH) method.

Fourier-transform infrared analysis

The Fourier-transform infrared (FTIR) spectra of the zeolite samples were recorded on a Thermo-Nicolet AVATAR 370 FTIR spectrometer.

Scanning electron microscopy analysis

The morphologies and sizes of the NaY zeolite crystals were determined using scanning electron microscopy (SEM; JEOL JSM-6360 microscope) after coating the samples with an Au evaporated film.

Results and discussion

Characterization of the intercalation composites

XRD analysis

The XRD traces of raw kaolin and kaolin/DMSO composites with various intercalation ratios are shown in Fig. 1. The 001 diffraction maximum of kaolinite at $2\theta = 12.4^\circ$ (0.72 nm) is displaced to $2\theta = 8.16^\circ$ (1.13 nm) in kaolin/DMSO intercalation composites (Fig. 1). In addition, progressive intercalation by DMSO decreased the intensity of the (001) peak at $2\theta = 12.4^\circ$ significantly, and the intensity of peak at $2\theta = 8.16^\circ$ increased gradually, suggesting that the intercalation of DMSO molecules in the kaolinite increased the distance between the kaolinite layers. This indicates that the periodic array of Al–O octahedra and Si–O tetrahedra along the c -axis was disrupted (Li *et al.*, 2007). The existence of the (001) peak at 0.72 nm indicates that intercalation of DMSO was not complete.

FTIR spectroscopy

Figure 2 shows the FTIR spectra of kaolin and KDM. The DMSO molecules have been intercalated into the kaolinite layers. Due to the chemical bond between kaolinite and DMSO, the position and intensity of the infrared absorption bands of the intercalation composites were affected. The 1043.21 cm^{-1} band due to Si–O stretching shifted to 1027.97 cm^{-1} . In addition, after intercalation, DMSO molecules entered the kaolinite layers, the bands at 758 and 694 cm^{-1} shifted to 749 and 689 cm^{-1} and their intensities slightly decreased. In contrast, the position and intensity of the OH stretching band of internal hydroxyls at 3620 cm^{-1} remained essentially unaffected.

SEM spectroscopy

Figure 3 shows the SEM micrographs of kaolin and KDM. Compared with kaolin, the particle size of KDM showed distinct changes. After intercalation, the particles became smaller and the amount of fine particles increased, which was advantageous to the dispersion. In addition, the pH value of kaolin slurry changed

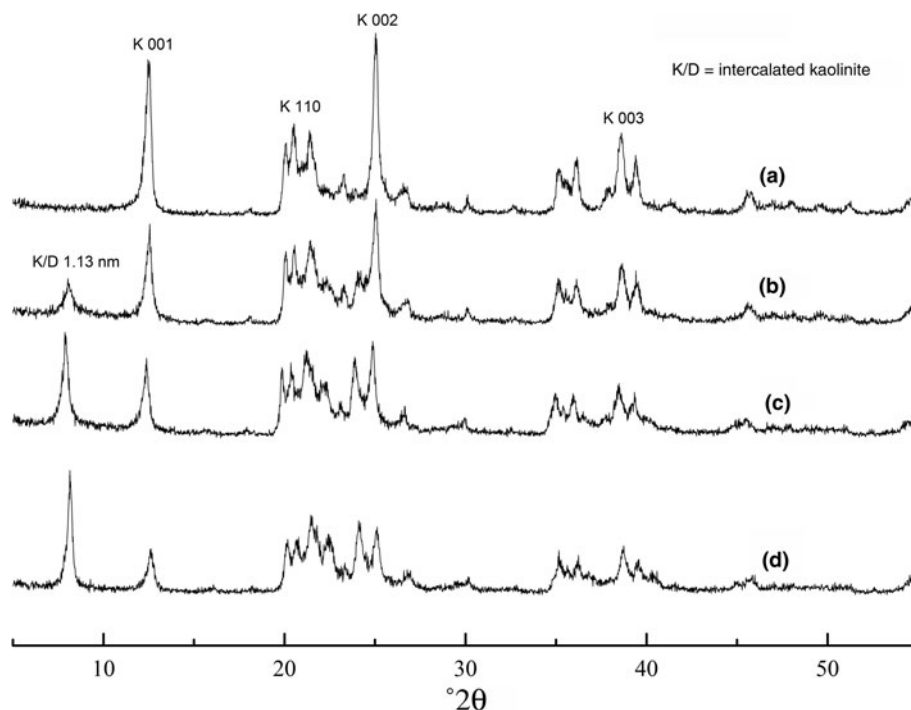


Fig. 1. XRD traces of samples with various intercalation ratios of (a) kaolin; (b) kaolin/DMSO, ratio 22%; (c) kaolin/DMSO, ratio 55%; and (d) kaolinite/DMSO, ratio 84%.

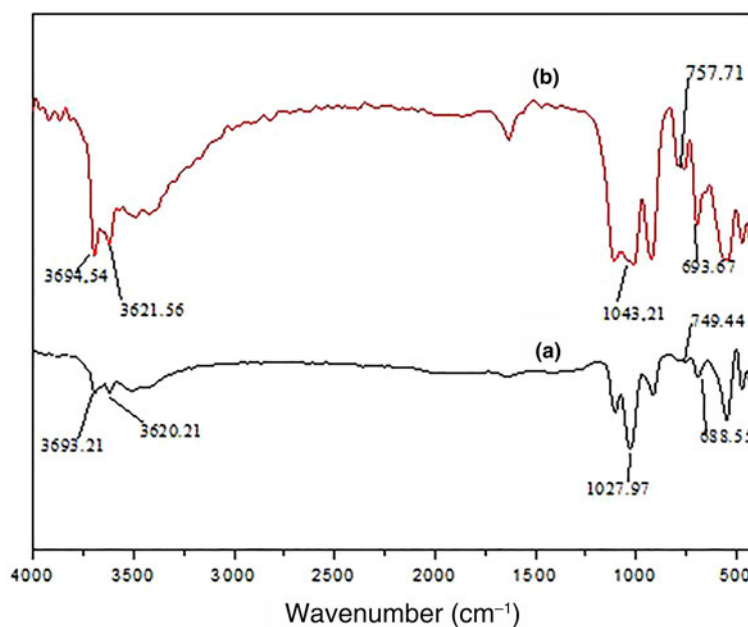


Fig. 2. FTIR spectra of (a) KDM and (b) kaolin.

from slightly acidic (6.12) in the original kaolin to slightly alkaline (7.68) in the kaolin/DMSO composite, leading to the increase of the solid content of kaolin particles with increasing pH value. Therefore, after intercalation, the dispersion of kaolin particles was improved, the viscosity of slurry decreased and the negative charges increased.

Pore structure

Figure 4 shows the N_2 adsorption–desorption isotherms and the pore-size distributions of kaolin and KDM. KDM showed a typical type IV adsorption–desorption isotherm. The hysteresis loop that occurred in the partial pressure range $0.80 < P/P_0 < 1.0$

was ascribed to the presence of mesopores and macropores. The hysteresis loop was of H3 hysteresis type, indicating that the material formed slit-shaped pores with the loose accumulation of platy particles. The pore-size distribution of KDM showed maxima at ~ 2.4 , 3.2, 4.0 and 30.0 nm, while the pore-size distribution of kaolin showed maxima at ~ 4.0 , 15.0 and 30.0 nm. These pore sizes indicate the existence of mesopores.

De-intercalation behaviour of the intercalation composite

During the synthesis of the NaY zeolite molecular sieve, the reaction temperature of the system was $\sim 100^\circ\text{C}$, and the intercalation

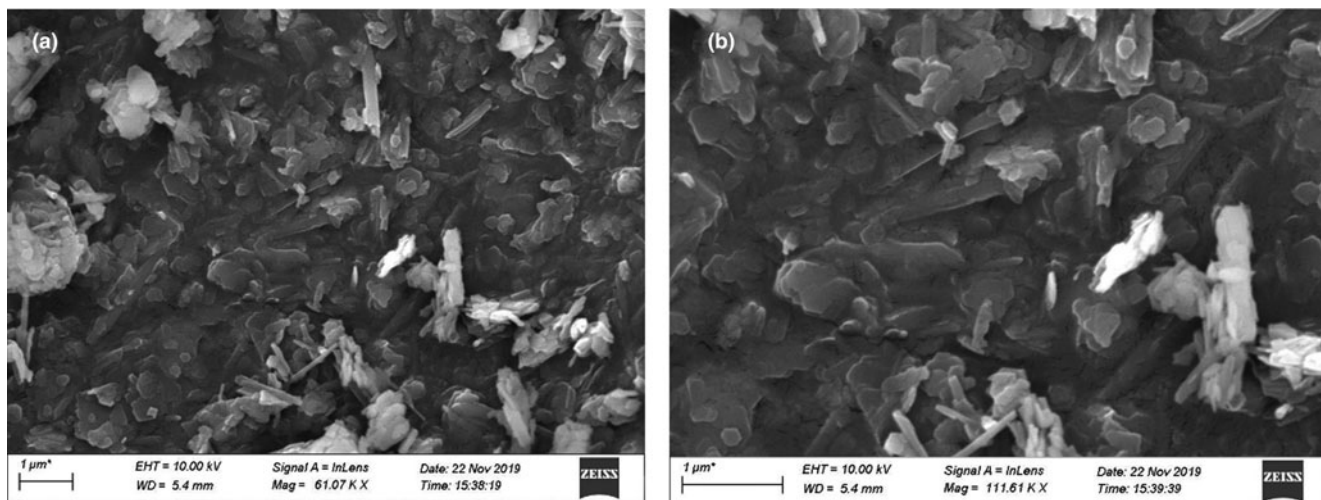


Fig. 3. SEM images of (a) KDM and (b) kaolin.

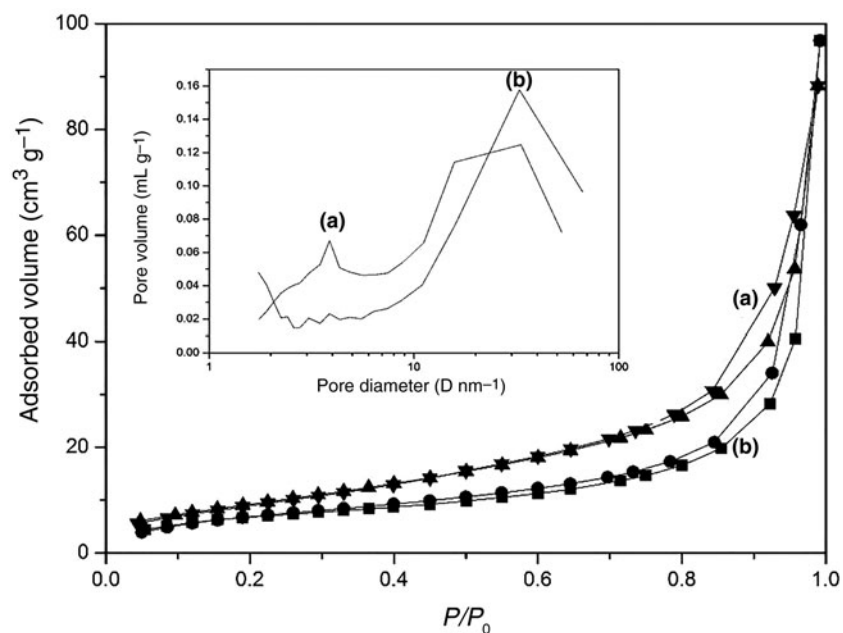


Fig. 4. N₂ adsorption-desorption isotherms and pore-size distributions of (a) kaolin and (b) KDM.

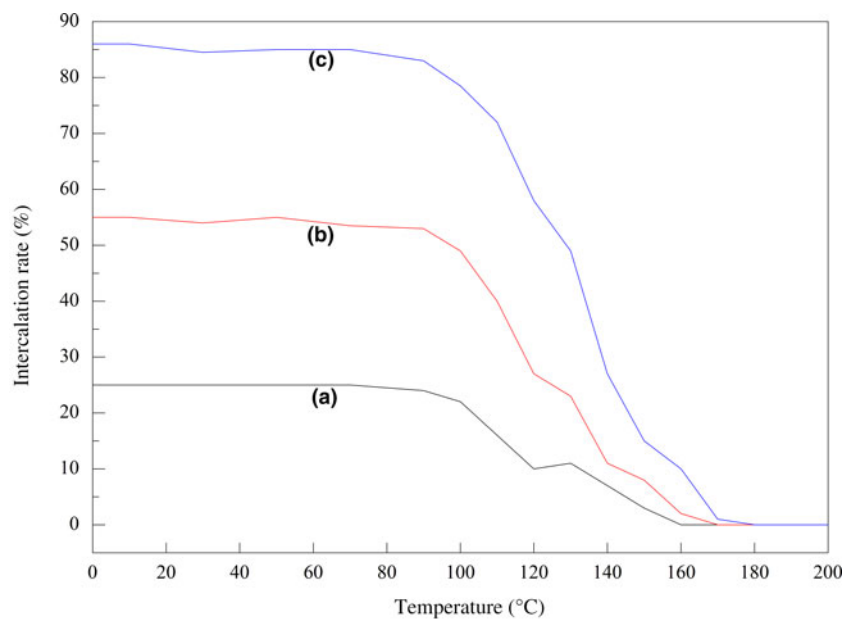


Fig. 5. The de-intercalation behaviour of KDM with various intercalation ratios of (a) 22%, (b) 55% and (c) 84%.

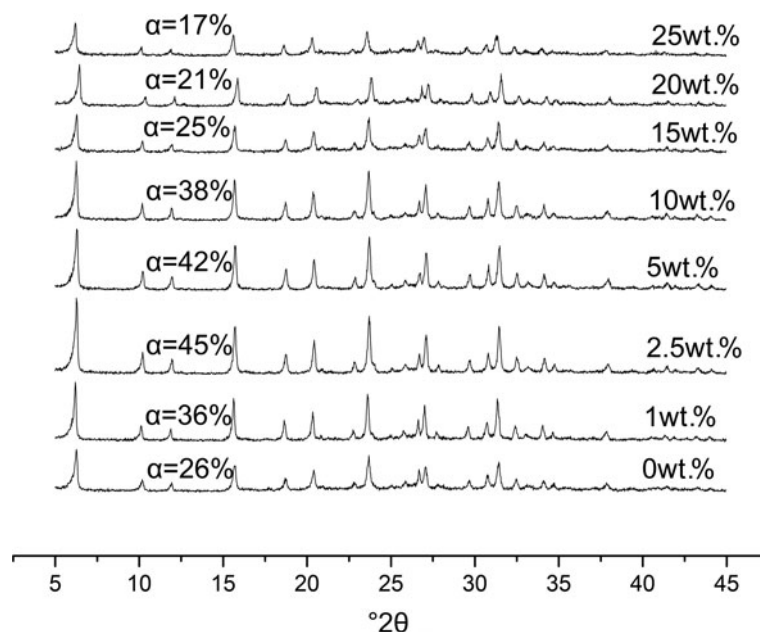


Fig. 6. XRD traces of NaY zeolites synthesized from KDM with an 84% intercalation ratio at various addition amounts.

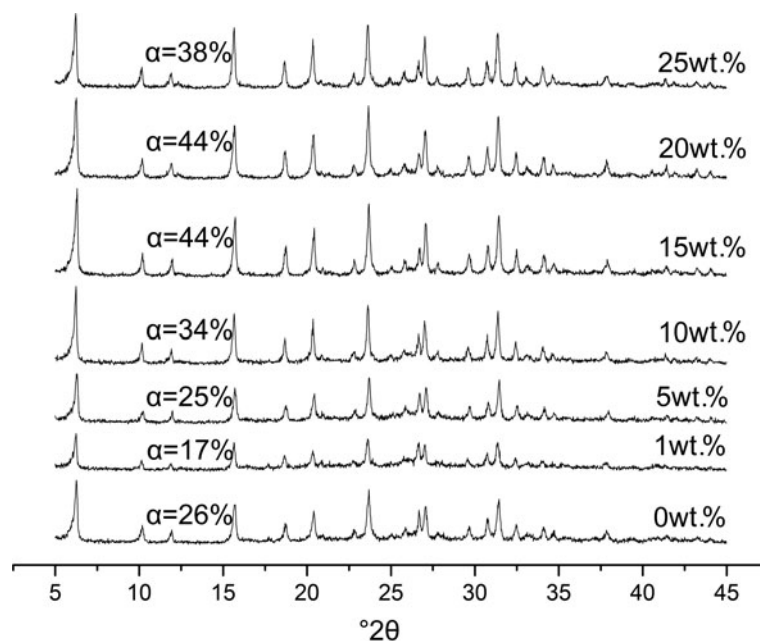


Fig. 7. XRD traces of NaY zeolites synthesized from KDM with a 55% intercalation ratio at various addition amounts.

composite was modified at this temperature. Figure 5 shows the de-intercalation behaviour of the intercalation composites with various intercalation ratios obtained at various temperatures. The de-intercalation behaviour of the KDM intercalation composite at various intercalation ratios essentially did not change. At temperatures $<80^{\circ}\text{C}$, there was no obvious change in the intercalation ratio of the composites, indicating a lack of de-intercalation. In the composite with an 84% intercalation ratio, the onset of de-intercalation occurred at temperatures $>80^{\circ}\text{C}$. In addition, the lower the intercalation ratio, the higher the de-intercalation temperature. Hence, in composites with 22% and 55% intercalation ratios, de-intercalation began at $\sim 100^{\circ}\text{C}$. When the temperature was increased to 160°C , samples with an intercalation ratio of 25%

were completely de-intercalated. The remaining KDM composites were completely de-intercalated at 170°C .

Properties of the synthesized NaY zeolite

XRD analysis

Figures 6–8 show the effects of various amounts of the added KDM intercalation composite with various intercalation ratios on the synthesis of NaY zeolite. The use of intercalation composites with various intercalation ratios clearly affected the NaY zeolite synthesis. The crystallinity of the NaY zeolite increased first and decreased thereafter with an increased amounts of added KDM. At an 84% intercalation ratio and 2.5 wt.% amount of

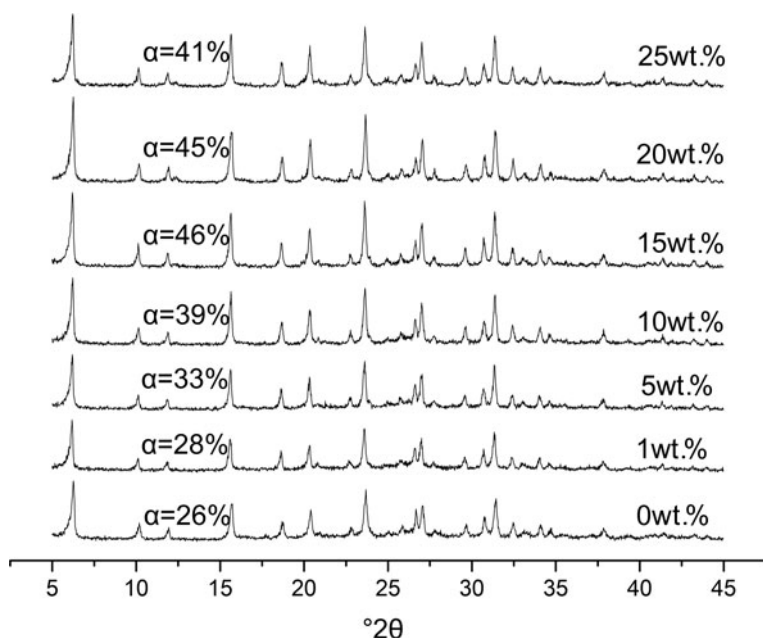


Fig. 8. XRD traces of NaY zeolites synthesized from KDM with a 22% intercalation ratio at various addition amounts.

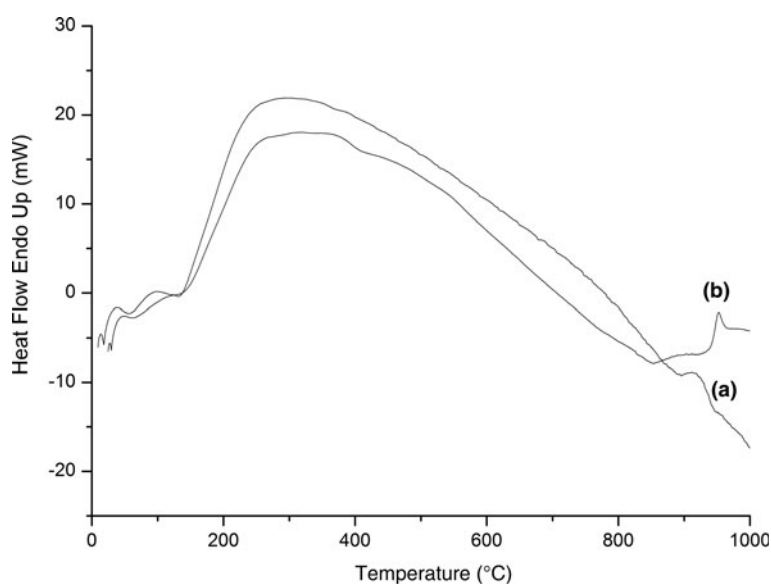


Fig. 9. DTA curves of synthesized NaY zeolites (a) R-NaY and (b) D-NaY.

added KDM, the crystallinity of the NaY zeolite was at a maximum, reaching $\sim 45\%$. The onset of the de-intercalation of KDM at an intercalation ratio of 84% occurred at $\sim 80^\circ\text{C}$. As the synthesis temperature was $\sim 100^\circ\text{C}$, the intercalation composite continued to be de-intercalated, consuming the heat energy of the system. Therefore, at this reaction temperature and reaction time, the KDM with higher intercalation ratios inhibited the synthesis of NaY zeolite. For intercalation ratios of 55% and 22% and amounts of added KDM at 15%, the crystallinities of NaY zeolite were 44% and 47%, respectively. Compared to the crystallization product without the addition of KDM, the crystallinity of the NaY zeolite increased by $>70\%$.

Differential thermal analysis

Figure 9 shows the differential thermal analysis (DTA) curves of NaY zeolite molecular sieves synthesized from KDM and from

pure kaolin. The DTA curves of the NaY zeolite are essentially identical, with a large endothermic peak at $\sim 300^\circ\text{C}$ due to the desorption of adsorbed water from the zeolite surface. The R-NaY molecular sieve displays an exothermic peak at $\sim 910^\circ\text{C}$ due to the recrystallization of kaolinite. The exothermic peak of D-NaY zeolite occurs at $\sim 930^\circ\text{C}$, which indicates that the intercalated NaY zeolite has higher thermal stability.

SEM analysis

Figure 10 shows SEM images of D-NaY and R-NaY zeolites. The NaY zeolite crystals mainly have a rhombohedral shape. The D-NaY zeolite crystals are $\sim 0.5\ \mu\text{m}$ in size, uniform and lack agglomeration (Fig. 10a,b). In contrast, the R-NaY zeolite crystals are heterogeneous in size and slightly larger than their D-NaY zeolite counterparts (Fig. 10c,d). The smaller particle size of the D-NaY zeolite indicates that the activity and the

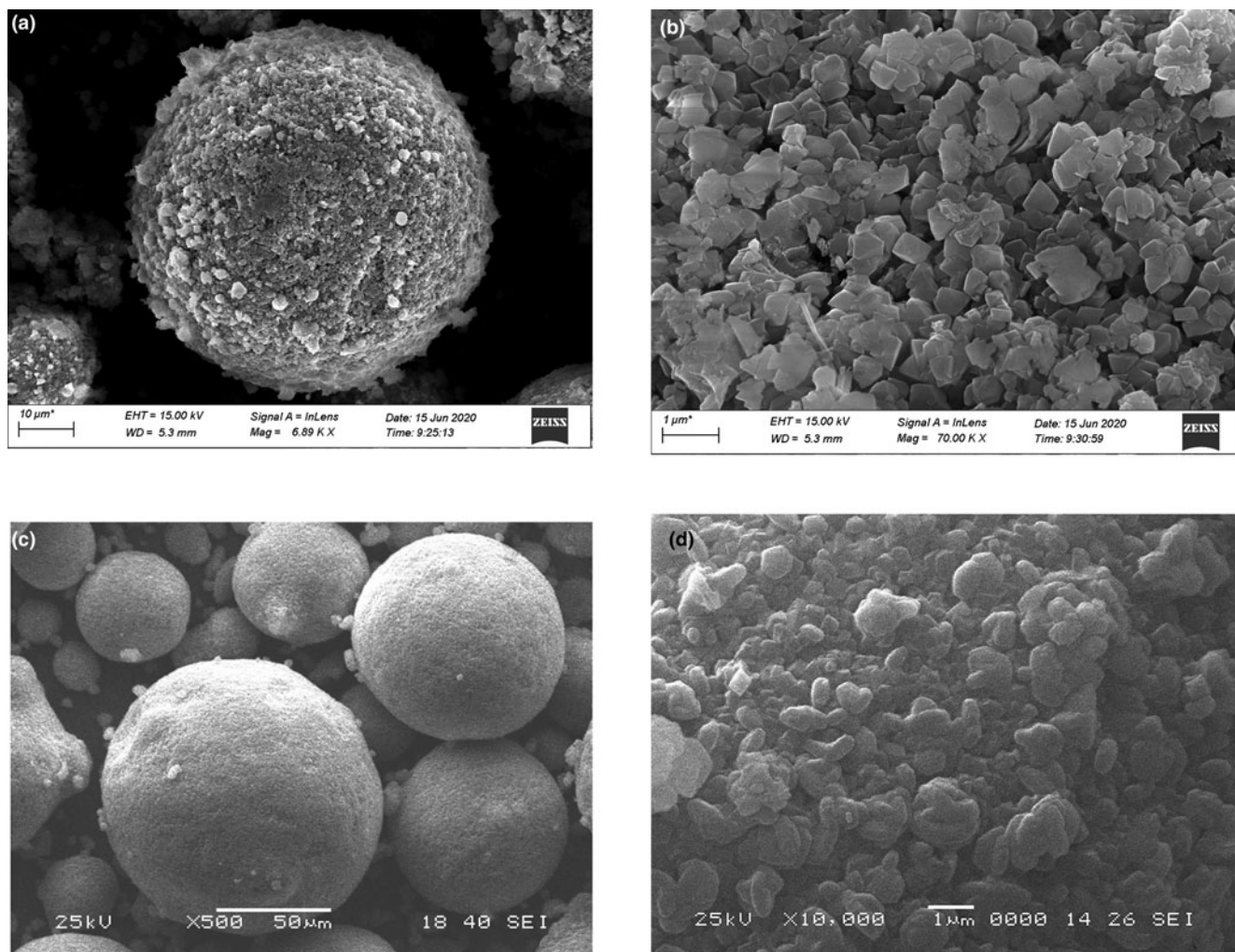


Fig. 10. SEM images of synthesized NaY zeolites (a, b) D-NaY and (c, d) R-NaY.

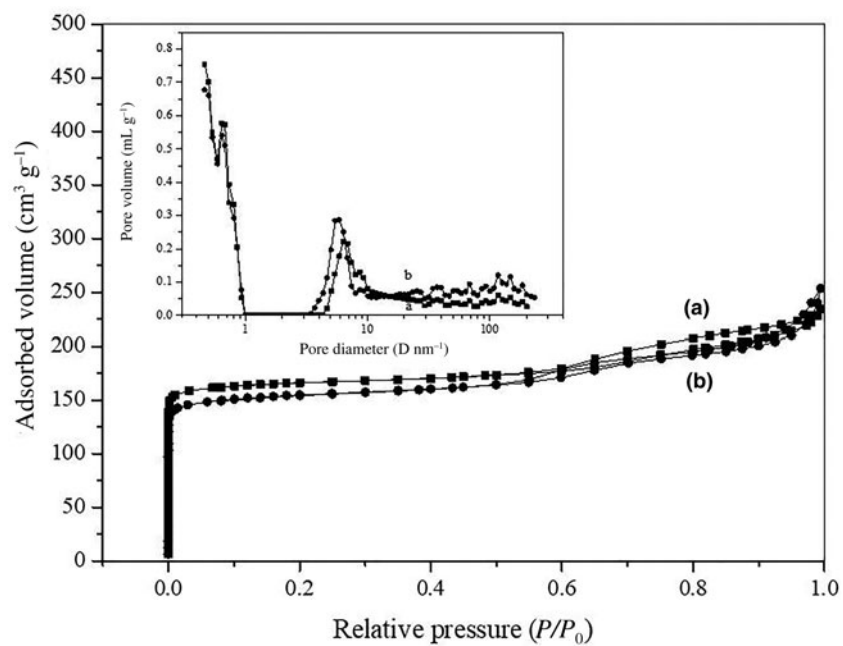


Fig. 11. N_2 adsorption-desorption isotherms and pore-size distributions of synthesized NaY zeolites (a) R-NaY and (b) D-NaY.

Table 1. BET specific surface areas and pore structures of the NaY zeolites.

	D-NaY	R-NaY
Average pore size (nm)	2.73	3.32
Total pore volume (cm ³ g ⁻¹)	0.355	0.392
Micropore volume (cm ³ g ⁻¹)	0.230	0.203
BET specific surface area (m ² g ⁻¹)	519	472
Micropore specific surface area (m ² g ⁻¹)	443	388

catalytic performance of this zeolite are better than those of the R-NaY zeolite. Hence, the intercalation composite is not only beneficial in terms of reducing the grain size and making the grains on the surface smoother, but it may also prevent the aggregation of NaY zeolite crystals during synthesis.

Pore structure

Figure 11 shows the N₂ adsorption–desorption isotherms and the pore-size distributions of the synthesized NaY zeolites. The zeolites exhibited typical adsorption behaviour of microporous materials with a type I isotherm. A sharp increase in nitrogen uptake at a relative low pressure was observed in the D-NaY and R-NaY zeolites, which may be ascribed to their microporosity. In addition, the adsorption isotherms of both zeolites showed that H1-type hysteresis exists in the range $0.50 < P/P_0 < 1.0$ due to the presence of mesopores. The synthesized NaY zeolites with a mesoporous pore structure showed greater performance and demonstrated wider applications. The mesoporosity in these samples is represented by the pore-size distribution from 3 to 70 nm with a peak at ~6 nm. Table 1 shows the BET specific surface areas and pore structures of the NaY zeolites. Compared with R-NaY molecular sieve, the BET specific surface area and the micropore specific surface area of D-NaY were increased by 47 and 55 m² g⁻¹, respectively. The larger the specific surface area, the stronger the adsorption capacity of the zeolites. Total pore volume decreased by 0.037 mL g⁻¹, but micropore pore volume increased by 0.027 mL g⁻¹. Finally, the average pore diameter was reduced by 0.6 nm. On the basis of the nitrogen adsorption characterization, it can be inferred that the D-NaY molecular sieve synthesized from kaolin/DMSO intercalation composite has greater mesoporosity.

Conclusions

NaY zeolite molecular sieves were synthesized using an *in situ* crystallization technique with a kaolin/DMSO intercalation composite. The kaolin/DMSO intercalation composites were prepared using the direct intercalation method. After intercalation, the kaolinite particles became smaller and the amount of fine particles increased. The intercalation composite with an 84% intercalation ratio began to de-intercalate at temperatures >80 °C and the intercalation composites with 22% and 55% intercalation ratios began to de-intercalate at ~100 °C. The optimum additional amount of kaolin/DMSO intercalation composite with an 84% intercalation ratio was 2.5%, yielding NaY zeolite with a crystallinity of 46%. The synthesized NaY zeolite had a particle diameter of 0.5 μm and a wide-pore structure, and it showed good thermal stability and a BET specific surface area and pore volume of 519 m² g⁻¹ and 0.355 mL g⁻¹, respectively.

Financial support. This work was financially supported by the National Natural Science Foundation of China (No.21371055), Key Project of Scientific Research Project of Hunan education department (No.18A313).

References

- Adams J.M. (1978) Differential scanning calorimetric study of the kaolinite: N-methylformamide intercalate. *Clay and Clay Minerals*, **26**, 169–172.
- Castrillo P.D., Olmos D. & González-Benito J. (2015) Kinetic study of the intercalation process of dimethylsulfoxide in kaolinite. *International Journal of Mineral Processing*, **144**, 70–74.
- Chen N.Y. & Garwood W.E. (1986) Industrial application of shape-selective catalysis. *Catalysis Reviews – Science and Engineering*, **28**, 185–264.
- Chen Y., Han D., Zhang Q. & Cui H. (2020) *In-situ* synthesis of hierarchical lamellar ZSM-5 zeolite with enhanced MTP catalytic performance by a facile seed-assisted method. *Journal of Porous Materials*, **27**, 1265–1275.
- Cheng H., Hou X., Liu Q., Li X. & Frost R.L. (2015) New insights into the molecular structure of kaolinite–methanol intercalation complexes. *Applied Clay Science*, **109–110**, 55–63.
- Cheng H., Liu Q., Cui X., Zhang Q., Zhang Z. & Frost R.L. (2012) The thermal behavior of kaolinite intercalation complexes—a review. *Thermochim Acta*, **545**, 1–13.
- Cheng H., Liu Q., Xu P. & Hao R. (2018) A comparison of molecular structure and deintercalation kinetics of kaolinite/quaternary ammonium salt and alkylamine intercalation compounds. *Journal of Solid State Chemistry*, **268**, 36–44.
- Cheng H., Liu Q., Yang J., Du X. & Frost R.L. (2010) Influencing factors on kaolinite potassium acetate intercalation complexes. *Applied Clay Science*, **50**, 476–480.
- Frost R.L., Kristof J. & Paroz G.N. (1998) Modification of the kaolinite hydroxyl surfaces through intercalation with potassium acetate under pressure. *Journal of Colloid and Interface Science*, **208**, 478–486.
- Harding R.H., Peters A.W. & Nee J.R.D. (2001) New developments in FCC catalyst technology. *Applied Catalysis A: General*, **221**, 389–396.
- Itagaki T., Komori Y., Sugahara Y. & Kuroda K. (2001) Synthesis of a kaolinite–poly(β-alanine) intercalation compound. *Journal of Materials Chemistry*, **11**, 3291–3295.
- Kovács A. & Makó É. (2016) Cooling as the key parameter in formation of kaolinite–ammonium acetate and halloysite–ammonium acetate complexes using homogenization method. *Colloids and Surfaces A: Physicochemical and Engineering Aspects*, **508**, 70–78.
- Kristóf T., Sarkadi Zs., Ható Z. & Rutkai G. (2018) Simulation study of intercalation complexes of kaolinite with simple amides as primary intercalation reagents. *Computation Materials Science*, **143**, 118–125.
- Kuroda K., Hiraguri K., Komori Y., Sugahara Y., Kuroda K., Komori Y. *et al.* (1999) An acentric arrangement of p-nitroaniline molecules between the layers of kaolinite. *Chemical Communications*, **22**, 2253–2254.
- Ledoux R.L. & White J.L. (1966) Infrared studies of hydrogen bonding interaction between kaolinite surfaces and intercalated potassium acetate, hydrazine, formamide, and urea. *Journal of Colloid and Interface Science*, **21**, 127–152.
- Li X., Cui X., Wang S., Wang D., Li K., Liu Q. & Komareni S. (2017) Methoxy-grafted kaolinite preparation by intercalation of methanol: mechanism of its structural variability. *Applied Clay Science*, **137**, 241–248.
- Li Z.J., Zhang X.R. & Xu Z. (2007) Novel method for preparation of kaolinite intercalation composite. *Materials Technology*, **22**, 205–208.
- Makó É., Kovács A., Ható Z., Zsirka B. & Kristóf T. (2014) Characterization of kaoliniteammonium acetate complexes prepared by one-step homogenization method. *Journal of Colloid and Interface Science*, **431**, 125–131.
- Makó É., Kovács A., Katona R. & Kristóf T. (2016) Characterization of kaolinite–cetyltrimethylammonium chloride intercalation complex synthesized through eco-friendly kaolinite–urea pre-intercalation complex. *Colloids and Surfaces A: Physicochemical and Engineering Aspects*, **508**, 265–273.
- Matsumura A., Komori Y., Itagaki T., Sugahara Y. & Kuroda K. (2001) Preparation of a kaolinite–nylon 6 intercalation compound. *Bulletin of the Chemical Society of Japan*, **74**, 1153–1158.
- Matusik J. & Klapyta Z. (2013) Characterization of kaolinite intercalation compounds with benzylalkylammonium chlorides using XRD, TGA/DTA and CHNS elemental analysis. *Applied Clay Science*, **83–84**, 433–440.
- Olejnik S., Aylmore L.A.G., Posner A.M. & Quirk J.P. (1968). Infrared spectra of kaolin mineral–dimethyl sulfoxide complexes. *Journal of Physical Chemistry*, **72**, 241–249.

- Qiu B., Jiang F., Lu W., Yan B., Li W.-C., Zhao Z.-C. & Lu A.-H. (2020) Oxidative dehydrogenation of propane using layered borosilicate zeolite as the active and selective catalyst. *Journal of Catalysis*, **385**, 176–182.
- Sang Y. & Li H. (2019) Effect of phosphorus and mesopore modification on the HZSM-5 zeolites for *n*-decane cracking. *Journal of Solid State Chemistry*, **271**, 326–333.
- Tsunematsu K. & Tateyama H. (1999) Delamination of urea-kaolinite complex by using intercalation procedures. *Journal of the American Ceramic Society*, **82**, 1589–1591.
- Valaskova M., Rieder M., Matejka V., Capkova P. & Sliva A. (2006) Exfoliation/delamination of kaolinite by low-temperature washing of kaolinite-urea intercalates. *Applied Clay Science*, **35**, 108–118.
- Wang P., Shen B.J. & Gao J.S. (2007) Synthesis of MAZ/ZSM-5 composite zeolite and its catalytic performance in FCC gasoline aromatization. *Catalysis Communications*, **8**, 1161–1166.
- Xiong K., Lu C., Wang Z. & Gao X. (2015) Kinetic study of catalytic cracking of heavy oil over an *in-situ* crystallized FCC catalyst. *Fuel*, **142**, 65–72.
- Yue Y., Guo X., Liu T., Liu H., Wang T., Yuan P. *et al.* (2020) Template free synthesis of hierarchical porous zeolite Beta with natural kaolin clay as alumina source. *Microporous and Mesoporous Materials*, **293**, 109772.
- Zhang Y., Kang W., Han H., Wang H., Chen Y., Gong X. *et al.* (2019) *In-situ* synthesis of NaP zeolite doped with transition metals using fly ash. *Journal of the American Ceramic Society*, **102**, 7665–7677.